Computational Antioxidant Capacity Simulation (CAOCS) Assay of Catechol, Resorcinol and Hydroquinone

Sunday Olakunle Idowu* and Morenikeji Ayodele Adeyemo

Department of Pharmaceutical Chemistry, Faculty of Pharmacy, University of Ibadan, Ibadan, Nigeria

Abstract: There is an urgent need for a biorelevant antioxidant capacity assay, which is crucial to quality-assured polyphenol dietary supplements. We hypothesize that the 'position', more than the 'number' of phenolic groups, is critical to the antioxidant capacity of polyphenols. Computational Antioxidant Capacity Simulation (CAOCS) assay was implemented to test the hypothesis, while refinement of existing assay protocol was aimed at reducing the cost of analysis. The antioxidant capacities of resorcinol, catechol and hydroquinone (3 diphenol positional isomers) were determined by CAOCS assay. Photometric titration experiments and associated informatics that constitute CAOCS assay were evaluated through the use of small increments (< 1 mL) of antioxidant solution. Antioxidant capacity ranking of the positional isomers was found to be; hydroquinone > catechol > resorcinol, (60/g, 46/g and 28/g respectively). The relative bond strength of the phenolic groups, which governs the ranking, was accounted for by structural theory. Optimal 250 µL increment of antioxidant solution afforded a 75% reduction of the amount of antioxidant required in the original assay protocol, where a 1 mL increment was used. CAOCS values vary widely for the positional isomers. The unique structure-antioxidant capacity-correlation (SACC) which confirmed our hypothesis is a signature of biorelevance. Significantly, microliter increments reduced the amount of active material required and hence, the cost of analysis. The methodology is thus attractive for profiling exotic and more expensive polyphenols. CAOCS assay holds a great promise of enabling quality-by-design (QbD) of polyphenol dietary supplements.

Keywords: Diphenol positional isomers, antioxidant capacity, photometric titration, model fitting, hydroquinone, biorelevant assay.

INTRODUCTION

The International Union of Pure and Applied Chemistry (IUPAC) recently reported that there is no official antioxidant capacity assay for food labeling. This is due to lack of standard quantification procedures in the various reported assay methodologies [1]. Similarly, the United States Department of Agriculture (USDA), after years of tacit endorsement [2], withdrew from their Nutrient Data Laboratory (NDL) website, database of values obtained from a particular antioxidant assay, Oxygen Radical Absorbance Capacity (ORAC), for selected dietary supplements. They cited as reason; "mounting evidence that the values indicating antioxidant capacity have no relevance to the effects of specific bioactive compounds, including polyphenols, on human health [3]. In other words, ORAC values are not considered biologically relevant, and do not indicate the potential of the antioxidants for health promotion.

The lack of biorelevance of results and standard quantification procedures means there is yet a gap in the quality assurance of manufactured dietary supplements. In an attempt to bridge this "biorelevance gap", a new assay was recently developed by Idowu & co-workers [4, 5]. Computational antioxidant capacity simulation (CAOCS) assay combines experimental data (obtained from proton transfer (PT) kinetics as a surrogate for hydrogen atom (HAT) transfer kinetics), and model fitting to create a systematic workflow that profiles the antioxidant capacity of polyphenol and phenol-like dietary supplements. The CAOCS assay algorithm consists of two photometric assays and associated informatics as depicted in the tree diagram shown in Figure **1**.

CAOCS assay was shown elsewhere (4) to satisfy several requirements for a biorelevant chemical assay. Notably, the CAOCS values reveal a strong correlation with a structural parameter that measures ionization constant and molecular electronic distribution (pKa). pKa governs solubility, permeability, absorption and receptor-binding of small molecule drugs and phytochemicals. In addition to bond dissociation energy (BDE), ionization potential (IP) also regulates hydrogen atom transfer (HAT), the process that underpins chain-breaking antioxidant action of phenolic compounds *in vivo*. Structure-antioxidant capacity-correlation (SACC) of CAOCS values is not just important; it is ultra unique to chemical assays for antioxidant capacity. It is a characteristic that was only previously reported for Electron Spin Resonance (ESR)-based method of antioxidant capacity profiling [6]. Structural theory considerations led to the hypothesis that the 'position', rather than just the 'number' of phenolic groups, predicts the antioxidant capacity of polyphenols. The high cost per gram of exotic polyphenols e.g. taxifolin,

*Correspondence Address to this author at the Department of Pharmaceutical Chemistry, Faculty of Pharmacy, University of Ibadan, Ibadan, Nigeria; Tel: +234 80 5842 7072; E-mail: olakunleid@yahoo.com

E-ISSN: 1929-5030/16

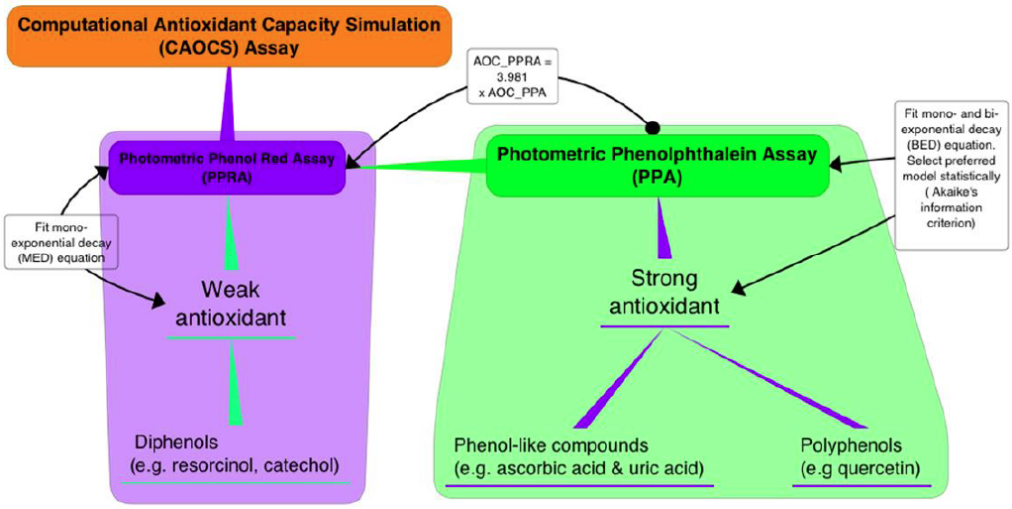

Figure 1: Tree diagram showing the systematic workflow of two photometric assays and associated informatics that constitute computational antioxidant capacity simulation (CAOCS) assay for polyphenols and phenol-like compounds.

also compelled a refinement of the previously documented CAOCS assay protocol, with the aim of reducing the cost of analysis.

This paper reports the antioxidant capacity of the three diphenol positional isomers (resorcinol, catechol and hydroquinone), as determined by CAOCS assay. These diphenols, except hydroquinone, are often found as fragments in the chemical structure of many antioxidant polyphenols (Figure **2**), while derivatives of hydroquinone are well reported as effective antioxidants [7, 8]. Small increments of antioxidant solution (< 1mL), in particular 250 and 500 µL were delivered from a micro-burette, instead of 1 mL increment from a standard burette in the photometric titration experiments. In consonance with our hypothesis; wide, structure-dependent variation in the CAOCS values obtained for the diphenol isomers, suggests the primacy of 'position' over 'number' of phenolic groups in predicting antioxidant capacity. A reliable low-cost assay protocol was also optimized for routine application.

MATERIALS AND METHODS

Chemicals and Reagents

Catechol (99%), resorcinol (99%) and hydroquinone (99%) were all from Sigma, U.S.A., sodium hydroxide, methanol (BDH, UK), phenol red (Kermel, China), phenolphthalein (BDH, U.K.).

Equipment

Digital colorimeter (Jenway, Model 6051, U.K), UV/Visible Spectrophotometer (Spectrumlab 752S, China), Analytical balance (Mettler, Toledo, PL203).

Preparation of Reagent and Test Solutions

Phenol Red Stock Solution (0.00625 % w/v)

Solution A (0.025 % w/v)

Phenol red (0.25 g) was weighed accurately into a beaker (50 mL) and dissolved in methanol with the aid of magnetic stirring. The solution was transferred into a volumetric flask (100 mL) and the solution was made up to mark with methanol.

Solution B (0.00625 % w/v)

Exactly 25 mL of Solution A of phenol red was pipetted into a volumetric flask (100 mL) and the solution was made up to mark with methanol (i.e. a 1 in 4 dilution).

Phenolphthalein Stock Solution (0.10 % w/v)

Phenolphthalein (0.10 g) was weighed and transferred into a beaker (50 mL) and dissolved in methanol with the aid of magnetic stirring. The solution was transferred into a volumetric flask (100 mL) and the solution was made up to mark with methanol.

Sodium Hydroxide Solution (0.025M and 0.01 M)

0.025 M Solution

Sodium hydroxide pellets (0.10 g) was weighed into a beaker (50 mL) and dissolved in distilled water with the aid of magnetic stirring. The solution was transferred into a volumetric flask (100 mL) and allowed to cool. The solution was afterwards made up to mark with distilled water.

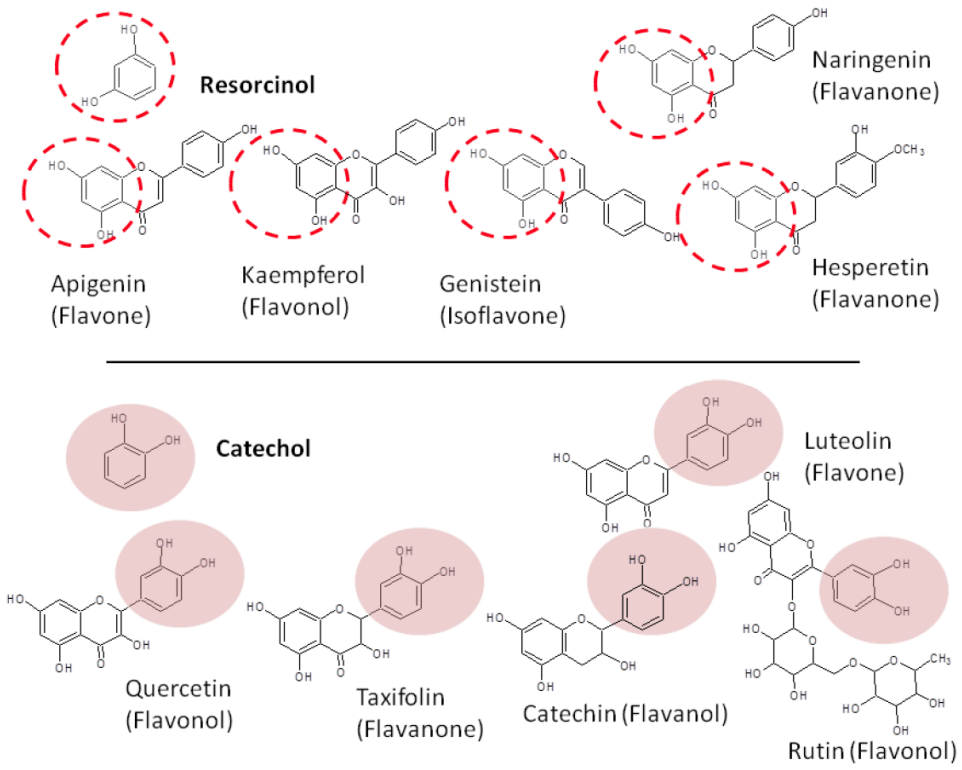

Figure 2: Chemical structures of antioxidant polyphenols having resorcinol and catechol fragment.

0.01 M Solution

An aliquot (40 mL) of the 0.025 M solution was pipetted into a volumetric flask (100 mL) and the solution was made up to mark with distilled water.

Photometric Phenol Red Assay (PPRA)

i) 500 µL Increment of Antioxidant Solution

Phenol red solution in methanol (1 mL, 0.00625% w/v) was pipetted into a volumetric flask (10 mL). To this was added sodium hydroxide solution in water (2 mL, 0.01 M) in order to generate the oxidized specie of the probe molecule. This solution was titrated by incremental addition of the test antioxidant solution (0.5 mL increment, up to a maximum of 3.5 mL), and the volume was made to mark with fresh methanol. The absorbance of the solution was measured at 540 nm on a digital colorimeter after each incremental addition. Each determination was performed in duplicate. A plot of absorbance against volume of titrant (antioxidant) was made and mono-exponential decay (MED) equation was fitted to the data.

a) Resorcinol Assay

The kinetic assay was performed as described above with standard solutions of resorcinol in methanol (1.0, 2.5, 5.0, 7.5 and 10.0 % w/v). The MED model was fitted by using the global curve-fitting method, in which plateau was shared and must be >0, the (proton transfer) reaction constant, k_{ptt}, was constrained to be >0. Regression coefficient, R^2 was computed for each standard solution and a global shared R^2 was also computed to show goodness-of-fit. Best-fit reaction constant was computed for each standard solution. A linear regression of the reaction constant versus concentration produced a slope which was used for computation of the antioxidant capacity (AOC).

b) Catechol Assay

The assay was performed as described above with standard solutions of catechol in methanol (0.5, 1.0, 2.5, 5.0 and 7.5% w/v). The MED model was fitted by using the global curve-fitting method as described under "resorcinol assay".

c) Hydroquinone Assay

The assay was performed as described above with standard solutions of hydroquinone in methanol (1.0, 2.5, 5.0, 7.5 and 10 % w/v). The MED model was fitted by using the global curve-fitting method as described under "resorcinol assay".

ii) 250 µL Increment of Antioxidant Solution

Phenol red solution in methanol (0.5 mL, 0.00625% w/v) was pipetted into a volumetric flask (5 mL). To this

was added sodium hydroxide solution in water (1 mL, 0.01 M) in order to generate the oxidized specie of the probe molecule. This solution was titrated by incremental addition of the test antioxidant solution (0.25 mL increment, up to a maximum of 1.75 mL), and the volume was made to mark with fresh methanol. The absorbance of the solution was measured at 540 nm on a digital colorimeter after each incremental addition. Each determination was performed in duplicate. A plot of absorbance against volume of titrant (antioxidant) was made and mono-exponential decay (MED) equation was fitted to the data.

a) Catechol Assay

The assay was performed as described above (cf. ii), with standard solutions of catechol in methanol (1.0, 2.0, 2.5, 5.0 and 7.5 % w/v). The MED model was fitted by using the global curve-fitting method as described under "resorcinol assay".

b) Resorcinol Assay

The assay was performed as described above (cf. ii), with standard solutions of resorcinol in methanol (1.0, 2.5, 5.0, 7.5 and 10 % w/v). The MED model was fitted by using the global curve-fitting method as described under "resorcinol assay".

Photometric Phenolphthalein Assay (PPA)

i) 500 µL Increment of Antioxidant Solution

Phenolphthalein solution in methanol (1 mL, 0.1% w/v) was pipetted into a volumetric flask (10 mL). To this was added sodium hydroxide solution in water (2 mL, 0.025 M) in order to generate the oxidized specie of the probe molecule. This solution was titrated by incremental addition of the test antioxidant solution (0.5 mL increment, up to a maximum of 3.5 mL), and the volume was made to mark with fresh methanol. The absorbance of the solution was measured at 540 nm on a digital colorimeter after each incremental addition. Each determination was performed in duplicate. A plot of absorbance against volume of titrant (antioxidant) was made and both bi-exponential (BED) model and mono-exponential decay (MED) model were fitted to the data. The preferred model was statistically selected after fit comparison, by using the Akaike's Information Criterion (AICc)

a) Hydroquinone Assay

The assay was performed as described above by using standard solutions of hydroquinone in methanol (0.5, 1.0, 2.5, 5.0 and 7.5 % w/v). The fit comparison was implemented by using global curve fitting method. For the BED model, plateau was shared and must be >0, k_1 and k_2 were constrained and must be > 0. For the MED model, plateau was shared and must be > 0, and k was constrained and must be > 0. (The curve fitting started with absorbance signal of the first increment, excluding the initial value of absorbance signal. This is peculiar to hydroquinone assay). The model with the highest "probability that it is correct" was selected as the preferred model. Regression coefficient, R^2 was computed for each standard solution and a global shared R^2 was also computed to show goodness-of-fit. Best-fit reaction constant was computed for each standard solution. A linear regression of the reaction constant versus concentration produced a slope which was used for computation of the antioxidant capacity (AOC). AOC on PPA platform was converted to the AOC on PPRA platform by a conversion factor.

ii) 250 µL Increment of Antioxidant Solution

Phenolphthalein solution in methanol (0.5 mL, 0.1% w/v) was pipetted into a volumetric flask (5 mL). To this was added sodium hydroxide solution in water (1 mL, 0.025 M) in order to generate the oxidized specie of the probe molecule. This solution was titrated by incremental addition of the test antioxidant solution (0.25 mL increment, up to a maximum of 1.75 mL), and the volume was made to mark with fresh methanol. The absorbance of the solution was measured at 540 nm on a digital colorimeter after each incremental addition. Each determination was performed in duplicate. A plot of absorbance against volume of titrant (antioxidant) was made and both bi-exponential (BED) model and mono-exponential decay (MED) model were fitted to the data. The preferred model was statistically selected after fit comparison by using the Akaike's Information Criterion (AICc)

a) Hydroquinone Assay

The assay was performed as described above (cf. ii) by using standard solutions of hydroquinone in methanol (1.0, 2.5, 5.0, 7.5 and 10.0 % w/v). The fit comparison was implemented by using global curve fitting method, as described under "hydroquinone assay" (cf. ia)

Investigation of Molecular Interaction between Probe Molecules and Hydroquinone

i) Data Visualization

The plot of absorbance against volume of hydroquinone solution (0.5 mL increment) was

compared by visualization of the data that make up the profile of hydroquinone on PPRA and PPA assay platforms.

ii) Overlay of Spectra - Catechol in PPRA

The absorption spectrum of phenol red reference solution made up to mark at the start of the photometric titration (i.e. 0 mL increment) was overlaid with the absorption spectrum of the test solution obtained with 0.5 mL increment of 1% w/v catechol solution in methanol. The scans were recorded from 200 - 700 nm.

iii) Overlay of Spectra - Hydroquinone in PPRA

The absorption spectrum of phenol red reference solution made up to mark at the start of the photometric titration (i.e. 0 mL increment) was overlaid with the absorption spectrum of the test solution obtained with 0.5 mL increment of 1% w/v hydroquinone solution in methanol. The scans were recorded from 200 - 700 nm.

iv) Overlay of Spectra - Hydroquinone in PPA

The absorption spectrum of phenolphthalein reference solution made up to mark at the start of the photometric titration (i.e. 0 mL increment) was overlaid with the absorption spectrum of the test solution obtained with 0.5 mL increment of 1% w/v hydroquinone solution in methanol. The scans were recorded from 200 - 700 nm.

v) Sample Visualization: Test Solutions of Catechol Versus Test Solutions of Hydroquinone in PPRA

Standard solution (1% w/v) of catechol and hydroquinone in methanol were prepared for PPRA. Test solutions were prepared as described above (PPRA ib & ic) with increments (0, 0.5, 1.0, and 2.0 mL). The colour of the solutions was inspected and the image acquired with a digital camera.

Mathematical Modeling and Statistical Analysis

Mono-exponential decay (MED) model

$$Absorbance = Ae^{-kV} + C \quad (1)$$

(A=Span, k= reaction constant, V= Volume of antioxidant, C= plateau)

Bi-exponential decay (BED) model

$$Absorbance = A_1e^{-k_1V} + A_2e^{-k_2V} + C \quad (2)$$

(A_1 = Span 1, A2 = Span 2, k1, K2 = reaction constants, V = volume of antioxidant, C= plateau)

Digital signal processing (DSP)

Digital signal processing of data was performed by using a complex multiplier, Kcf, which is different for each data set, to filter out random error:

$$K_{cf} = \frac{\left[\sum_{i=1}^{n} A_i\right] \Big/ n}{A_i} \quad (3)$$

(A_i = mean of initial absorbance values for each standard solution

n = number of standard solutions that makes up a family of data sets)

Calculation of AOC (/g)

The AOC metric was computed from the following relationship (4):

$$Slope = \frac{K_{ptt}(mL^{-1})}{Concentration(\%, w/v)} = \frac{mL^{-1}}{g \Big/ 100mL} = \frac{100}{g} \quad (4)$$

$$AOC = \frac{\left(Slope \times 100\right)}{g} \quad AOC_{PPRA} = 3.981 \times AOC_{PPA} \quad (5)$$

Akaike's information criterion

When there are several competing models, the Akaike's information criterion (AICc) is defined by the model and the maximum likelihood estimates of the parameters, which give the minimum of AICc defined by:

AIC = (-2) $\log_{10}$ (maximum likelihood) + 2(number of independently adjusted parameters)

The model with the lowest AIC value is the one that fits the data with minimum loss of information and hence with the highest "probability it is correct", which is thus selected as the preferred model [9].

All mathematical and statistical analyses were performed by GraphPad Prism version 4.03 for Windows (GraphPad Software, San Diego, CA, www.graphpad.com, 2005).

RESULTS

The proton transfer kinetics modeling (PTKM) and computation of antioxidant capacity (AOC) for

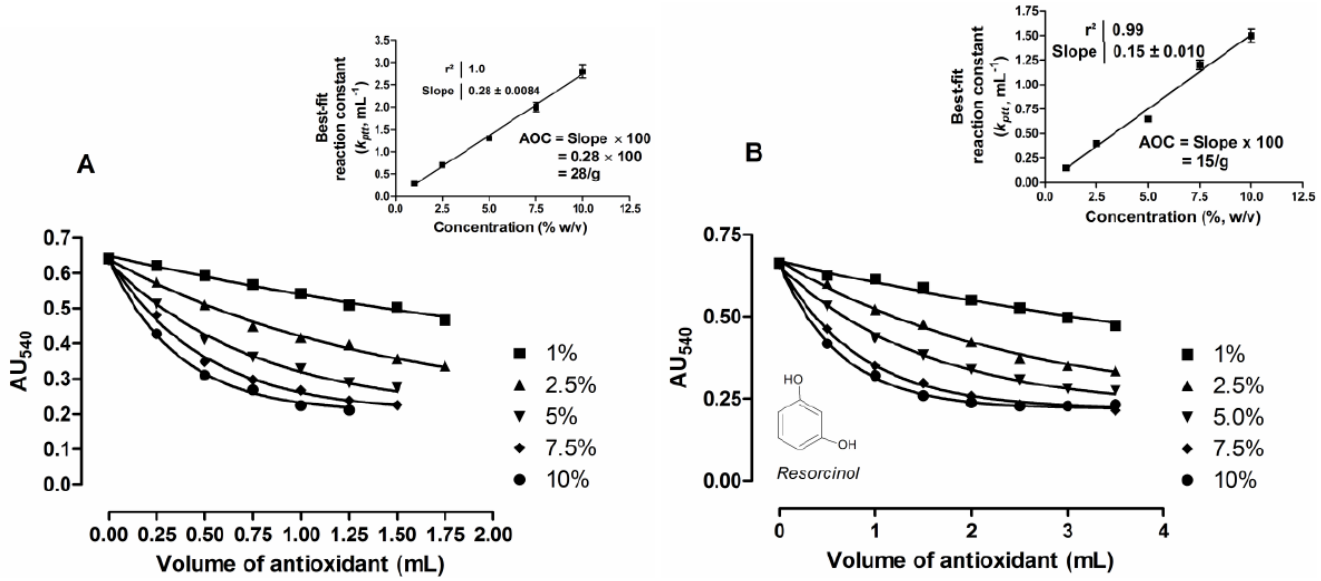

Figure 3: Kinetic data from standard solutions of resorcinol, on PPRA, showing (**A**) concentration- dependent response obtained from 250 µL incremental addition of antioxidant described by MED and the associated computation of antioxidant capacity, and (**B**) concentration-dependent response obtained from 500 µL incremental addition of antioxidant described by MED and the associated computation of antioxidant capacity.

Table 1: Model Parameters for CAOCS Assay (PPRA) of Resorcinol from a Global Fit of Classic Mono-Exponential Decay (MED), Using (a) 500 µL Increment, and (b) 250 µL Increment

Concentration (% w/v)	Best-fit values*	
	Proton transfer constant (k_{ptt}, mL^{-1} ± S.E.)	Regression coefficient (R^2)
a) 500 µL increment		
1.0	0.15 ± 0.0074	0.98
2.5	0.40 ± 0.013	0.99
5.0	0.65 ± 0.022	1.0
7.5	1.20 ± 0.049	1.0
10	1.50 ± 0.067	1.0
*Global shared parameters: R^2 =1.0, Plateau ± S.E = 0.22 ± 0.0036, Absolute sum of squares = 0.0018, $S_{y\times x}$ = 0.0079.		
b) 250 µL increment		
1.0	0.28 ± 0.016	0.99
2.5	0.70 ±0.028	1.0
5.0	1.30 ± 0.057	1.0
7.5	2.00 ± 0.10	1.0
10	2.80 ±0.15	1.0
*Global shared parameters:R^2= 1.0, Plateau ± S.E. = 0.20 ± 0.0061, Absolute sum of squares = 0.0017, $S_{y\times x}$ = 0.0083.		

resorcinol is displayed in Figure **3** and the model parameters are shown in Table **1**.

PTKM and computation of AOC for catechol (CTC) is displayed in Figure **4**, while the model parameters are shown in Table **2**.

Molecular behavior of hydroquinone (HQ) in PPRA shows the formation of charge-transfer (CT) complex, and deviation from typical concentration-dependent absorbance decay obtained with resorcinol and catechol (Figure **5A**), whereas, hydroquinone reveals a more typical concentration-dependent absorbance decay in PPA (Figure **5B**).

CT formation between phenol red (PR) and HQ is corroborated by a blood red test solution formed with incremental addition of HQ, and absorbance increase at 540 nm (Figure **6B**). Conversely, CTC shows absorbance decay at 540 nm in PPRA, and the shift in

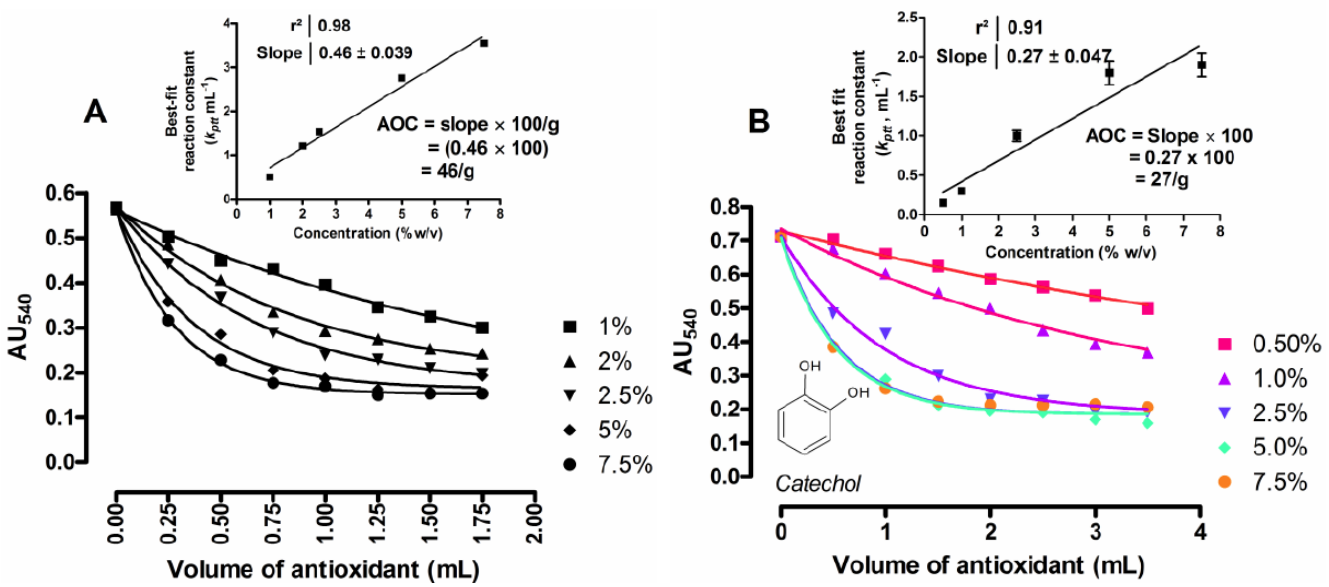

Figure 4: Kinetic data from standard solutions of catechol, on PPRA, showing (**A**) concentration-dependent response obtained from 250 µL incremental addition of antioxidant described by MED and the associated computation of antioxidant capacity, and (**B**) concentration-dependent response obtained from 500 µL incremental addition of antioxidant described by MED and the associated computation of antioxidant capacity.

Table 2: Model Parameters for CAOCS Assay (PPRA) of Catechol from a Global fit of Classic Mono-Exponential Decay (MED), Using (a) 500 µL Increment and (b) 250 µL Increment

Concentration (% w/v)	Best-fit values*	
	Proton transfer constant (k_{ptt}, mL^{-1} ± S.E.)	Regression coefficient (R^2)
a) 500 µL increment		
0.5	0.15 ± 0.014	0.98
1.0	0.30 ± 0.018	0.99
2.5	1.0 ± 0.068	0.98
5.0	1.8 ± 0.15	0.99
7.5	1.9 ± 0.50	0.99
*Global shared parameters: R^2 = 0.99, Plateau ± S.E.= 0.19 ± 0.0064, Absolute sum of squares = 0.0095, $S_{y\times x}$ = 0.018.		
b) 250 µL increment		
1.0	0.59 ± 0.032	0.99
2.0	1.0 ± 0.050	0.99
2.5	1.5 ± 0.075	1.0
5.0	2.6 ± 0.16	0.99
7.5	3.7 ± 0.26	1.0
*Global shared parameters: R^2 = 0.99, Plateau ± S.E. = 0.16 ± 0.0046, Absolute sum of squares = 0.0038, $S_{y\times x}$ = 0.011.		

equilibrium towards the acid form of PR is shown by gradual appearance of the yellow, acid color, in the initial pink, basic test solution (Figure **6A**).

HQ showed typical concentration-dependent behavior in PPA (Figure **7A**), through absorbance decay at 540 nm with incremental addition of HQ (Figure **6C**). Model parameters for PTKM of HQ in PPA are shown in Table **3**.

DISCUSSION

In the existing CAOCS assay protocol, 1 mL incremental addition of antioxidant solution was used,

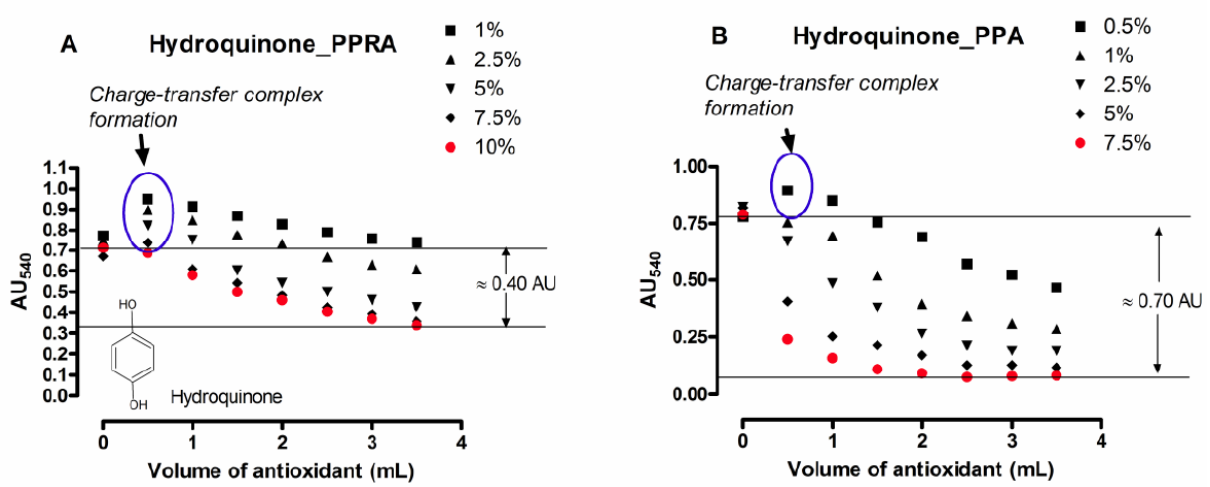

Figure 5: Kinetic data from standard solutions of hydroquinone on; (**A**) PPRA, showing a general pattern (except 10% solution) of initial increase in absorbance before commencement of decay. A difference of only 0.40 AU between initial absorbance and plateau suggests absorbance decay was limited even with the highest concentration. (**B**) PPA showing a slight increase in absorbance before commencement of decay, only for the more dilute solution (0.5%). A difference of 0.70 AU between initial absorbance and plateau suggests absorbance decay profile shows a typical concentration-dependent response.

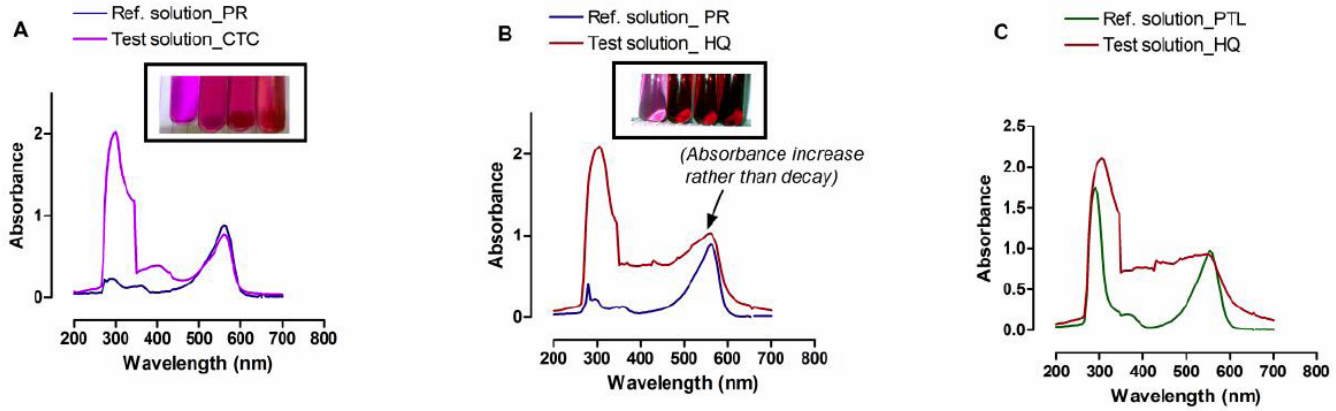

Figure 6: Overlay of absorption spectra of (**A**) reference phenol red (PR) solution and test solution obtained from 500 µL increment of 1% w/v catechol (CTC) solution in methanol, for PPRA, (**B**) reference PR solution and test solution obtained from 500 µL increment of 1% w/v hydroquinone (HQ) solution in methanol, for PPRA, (**C**) reference phenolphthalein (PTL) solution and test solution obtained from 500 µL increment of 1% w/v HQ solution in methanol, for PPA. HQ's behaviour in PPRA is anomalous, absorbance increase rather than decay at 540 nm, is suggestive of charge-transfer complex formation between HQ and phenol red. In contrast, HQ has little molecular interaction with PTL, spectral behavior of HQ in PPA bears resemblance to CTC in PPRA, (absorbance decay was induced at 540 nm).

Inset: Reference solution and test solution obtained by addition of 0.5, 1.0, and 2.0 mL of 1.0% w/v of: (**A**) catechol solution in methanol, showing a gradual shift of equilibrium and corresponding gradual appearance of yellow acid colour of phenol red in the initial pink, basic solution. (**B**) hydroquinone solution in methanol showing formation of blood red solution suggestive of molecular complexation between phenol red and benzoquinone.

up to a maximum of 7 mL for the two photometric assays [4] . This implies that the cost of analysis will be quite high for some exotic polyphenols e.g. taxifolin, which is over 1000 times the cost of naringenin per gram of substance. It was desirable therefore to investigate the use of smaller (< 1 mL) increments in the analysis. Second, the assay was shown to give a biorelevant output, through the strong correlation of CAOCS values with pKa, a structural parameter that measures the ionization potential of phenolic bonds and governs permeability and absorption of small molecules. It was desirable to further validate the biorelevant feature of the assay which was evidenced by structure-antioxidant capacity-correlation (SACC). Our hypothesis was that the 'number' of unsubstituted phenolic groups is not sufficient to predict the antioxidant capacity of a given polyphenol. Rather, the 'position' of the phenolic groups, i.e. the nature of the neighboring groups or chemical environment, will have a strong effect on the antioxidant capacity, in addition

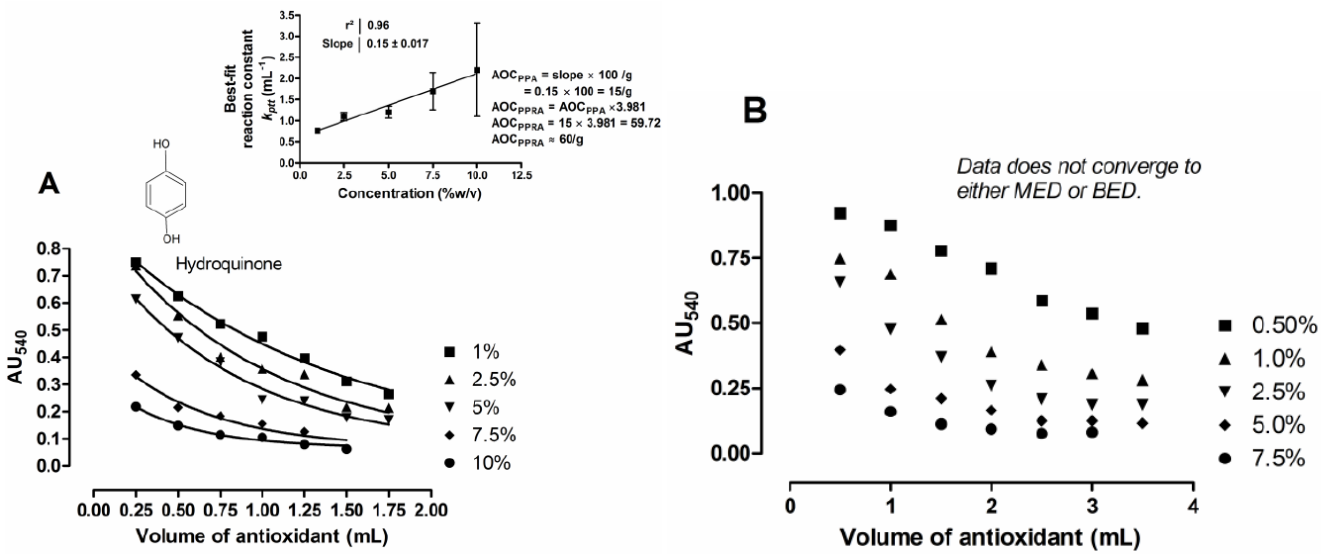

Figure 7: Kinetic data from standard solutions of hydroquinone, on PPA, showing (**A**) concentration-dependent response obtained from 250 µL incremental addition of antioxidant described by MED and the associated computation of antioxidant capacity, and (**B**) lack of convergence of data obtained from 500 µL incremental addition of antioxidant, when fitted with both MED and BED equations.

Table 3: Akaike Information Criterion (AICc) for Comparison and Selection of Preferred Model between Mono-Exponential Decay (MED) and Bi-Exponential Decay (BED) Fit for CAOCS (PPA) Assay of Hydroquinone Using 250 µL Increment

Comparison of fits	250 µL increment	500 µL increment
Simpler model	Mono-exponential decay	Data does not converge with either MED or BED
Probability it is correct	>99.99%	
Alternative model	Bi-exponential decay	
Probability it is correct	<0.01%	
Preferred model	Mono-exponential decay	
Difference in AICc	-97	
250 µL increment.		
Concentration (%w/v)	**Best-fit values***	
	Proton transfer reaction constant, (k_{ptt}, mL^{-1} ± S.E.)	**Regression Coefficient (R^2)**
1.0	0.77 ± 0.065	0.99
2.5	1.10 ± 0.098	0.97
5.0	1.20 ± 0.14	0.98
7.5	1.70 ± 0.44	0.95
10.0	2.20 ± 1.10	0.98

*Global shared parameters:
Plateau = 0.065 ±0.023, R^2 = 0.99, Absolute sum of squares = 0.012, $S_{y\times x}$ = 0.023.

to the number of phenolic groups. In order to test this hypothesis, we implemented CAOCS assay for a small chemical library of diphenols that are positional isomers, as model phenolics. The three candidates, resorcinol, catechol and hydroquinone all have two phenolic groups, positioned 1, 3; 1, 2; and 1, 4; respectively. Appropriate concentration range of the antioxidants were identified and investigated through incremental addition of 250 µL of the antioxidant, up to a maximum of 1.75 mL. In the second protocol, 500 µL increments of antioxidant solutions were added up to a maximum of 3.50 mL. PPRA was implemented for both

resorcinol (RES) and catechol (CTC), and MED model was fitted to the data. The AOC was computed as shown; for RES (Figure **3**) and CTC (Figure **4**). It was observed that the computed AOC value was higher for the experiments that used 250 µL increments in both cases. AOC values of 28/g and 46/g were obtained for resorcinol and catechol respectively. In essence, the assay protocol that afforded a cheaper cost of analysis was also the more accurate.

The main difference in the test solutions prepared when 250 µL increments was used is the smaller final volume (5 mL instead of 10 mL), the smaller relative amounts of oxidant, probe and antioxidant, and the smaller maximum volume of titrant (1.75 mL instead of 3.50 mL). These differences would lead to lower viscosity of the test solutions, constant refractive index and molar absorptivity. These considerations would contribute to greater photometric accuracy [10]. In addition, working with 250 µL increments always gave a larger value for the best-fit reaction constant (Tables **1** and **2**), which led to a higher value for the slope and hence, the computed AOC.

For HQ assay, it was observed during data collection, that the test solution in PPRA deepened and gave a blood red color during the photometric titration, in contrast to the gradual appearance of light yellow color within the initial pink solution, for RES and CTC. In addition, a poor sensitivity was observed for HQ assay in PPRA. A small difference of 0.40 AU was obtained between the initial absorbance reading and the plateau produced by the highest concentration investigated (Figure **5A**). HQ behaved differently in PPA, with a higher sensitivity, shown by a difference of 0.70AU between initial absorbance and plateau. A typical concentration-dependent response was also evident (Figure **5B**). The blood red color formed by HQ in PPRA is presumably due to charge-transfer (CT) complex formation between benzoquinone, which is produced alongside hydrogen transfer by HQ, and the probe molecule, Phenol red (Figure **8**). Benzoquinone is a *pi*-deficient aromatic compound and as such serves as electron acceptor. The formation of a molecular complex, quinhydrone, between mixture of equimolar quantities of alcoholic solution of hydroquinone and benzoquinone is well-known [11].

The chemical equilibrium of the phenolic probes shows that phenol red, unlike phenolphthalein, exists as a charged molecule (zwitterion) at very low pH (Figure **9**). In an alkaline solution, the type encountered at the start of the photometric titrations, phenolphthalien have the charged species being a phenolate and carboxylate. In contrast, phenol red has the charged species as phenolate and sulphonate. Carboxylate is a much stronger conjugate base than sulphonate, therefore, proton transfer more readily

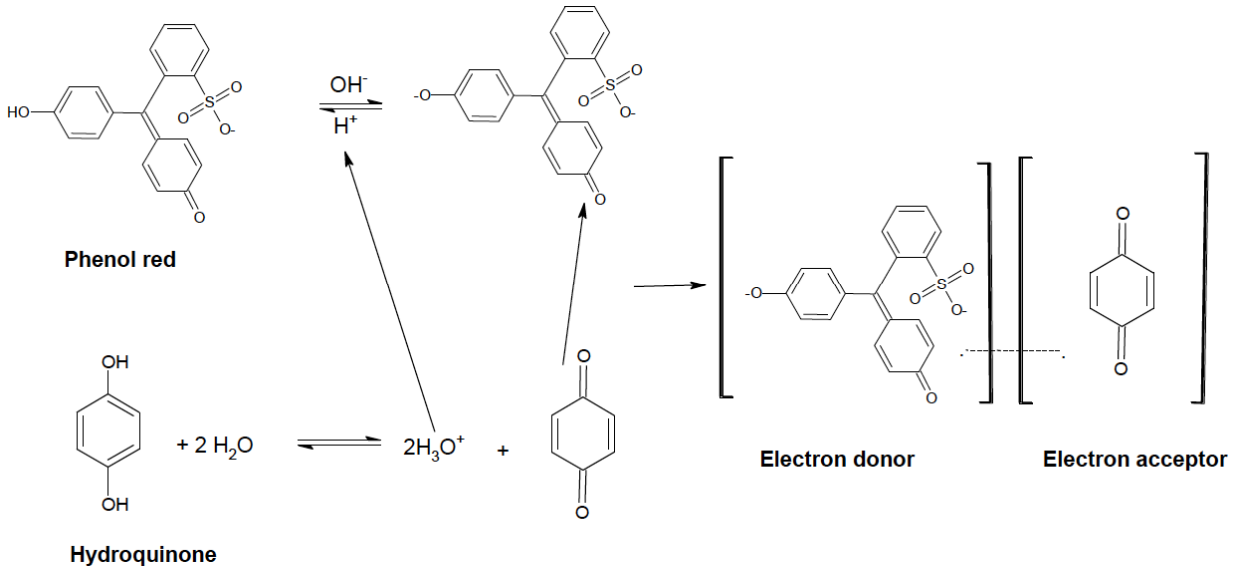

Figure 8: Formation of charge-transfer (CT) complex between oxidized phenol red and benzoquinone. Oxidized phenol red serves as the electron donor, while benzoquinone is the electron-acceptor. The complex formation is in competitive kinetics with the proton-induced reduction of the oxidized phenol red to form the partially ionized form of the probe molecule. As such, the CT complex formation is favoured when a small increment of hydroquinone is added (i.e. small proton concentration) to the analytical system containing oxidized phenol red. Phenol red forms a stronger CT complex, than phenolphthalein does with benzoquinone . This molecular interaction explains the initial absorbance increase before commencement of decay in the photometric phenol red assay of hydroquinone.

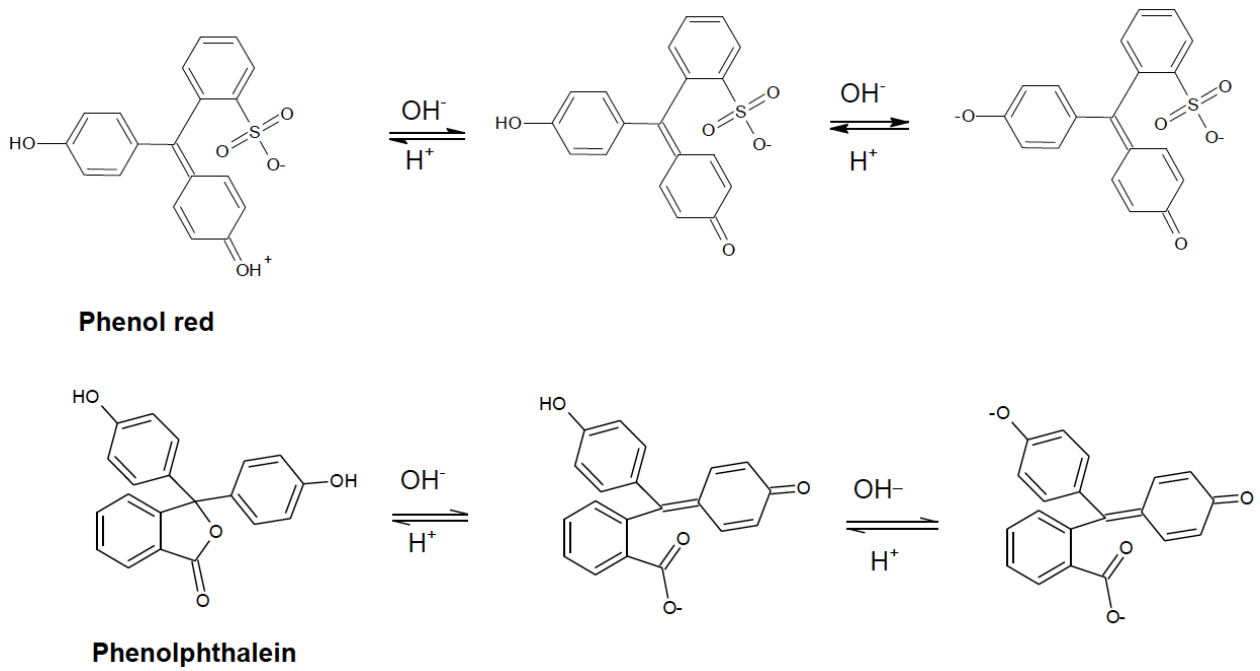

Figure 9: Ionization of phenolic probes showing chemical equilibrium between ionized and unionized (partially ionized) forms. Absorbance decay is induced by incremental addition of antioxidant with the accompanying proton transfer leading to progressive formation of the acidic form of the probes that exhibit lower molar absorptivity. Phenol red exists as zwitterion at very low pH, with the phenone group in the structure bearing a positive charge. Unlike phenolphthalein, phenol red remains a charged molecule in strongly acidic medium.

shifts the equilibrium towards the formation of the unionized specie of phenolphthalein (recombination of carboxylate with proton) [12]. On the other hand, there is a competitive kinetics that favors complex formation between benzoquinone and fully oxidized phenol red over proton-induced shift of equilibrium to the partially ionized specie, because of the slow acid-base reaction of the weakly basic sulphonate on phenol red molecule. The relative reactivity of carboxylate and sulphonate towards proton ensures that a more stable CT complex is formed between benzoquinone and phenol red than between benzoquinone and phenolphthalein [11].

The nature of intermolecular interaction involved in the assays was investigated by spectrophotometric measurements. Absorption spectra of the blood red test solution formed by HQ in PPRA relative to the reference solution, containing only the probe at the start of the titration, showed that there is an increase in absorbance at 540 nm (Figure **6B**), thus supporting the proposed complex formation. In contrast, HQ in PPA showed absorbance decay at 540 nm, of test solution relative to the reference solution (Figure **6C**). Absorbance decay at 540 nm was also found in the test solution produced by CTC in PPRA (Figure **6A**). Evidence of absorbance decay with a small increment (0.5 mL) of a dilute solution (1% w/v) will ensure good sensitivity of the assay procedure through a linear concentration-dependent detector response. Therefore, the assay of HQ could not be reliably performed on PPRA platform. PPA was adopted, using both 250 and 500 µL increments. The model fitting excluded the initial absorbance reading because absorbance increase was observed, when the first increment was added from the more dilute antioxidant solutions. MED and BED models were both fitted to the data, and the preferred model was selected by using Akaike's Information Criterion. MED was found as the preferred model for fitting the data obtained with 250 µL increments (Table **3**, Figure **7A**). The computed AOC gave a value of 60/g, after appropriate correction to harmonize the results with the PPRA platform. Neither MED nor BED model could fit the data obtained with 500 µL increment of antioxidant solutions (Figure **7B**).

The antioxidant capacity of the diphenol isomers therefore follow the sequence; hydroquinone > catechol > resorcinol (60/g, 46/g, 28/g respectively). This sequence can be accounted for through the structural theory lens. The three diphenols ionizes in an aqueous solution to form hydroxonium ion and a conjugate base (Figure **10**). Hydroquinone gave the highest AOC because the phenolic bonds are much weaker and are readily cleaved to form the resonance-stabilized, uncharged molecule, benzoquinone. The 1, 4 configuration of the two phenolic groups is critical to

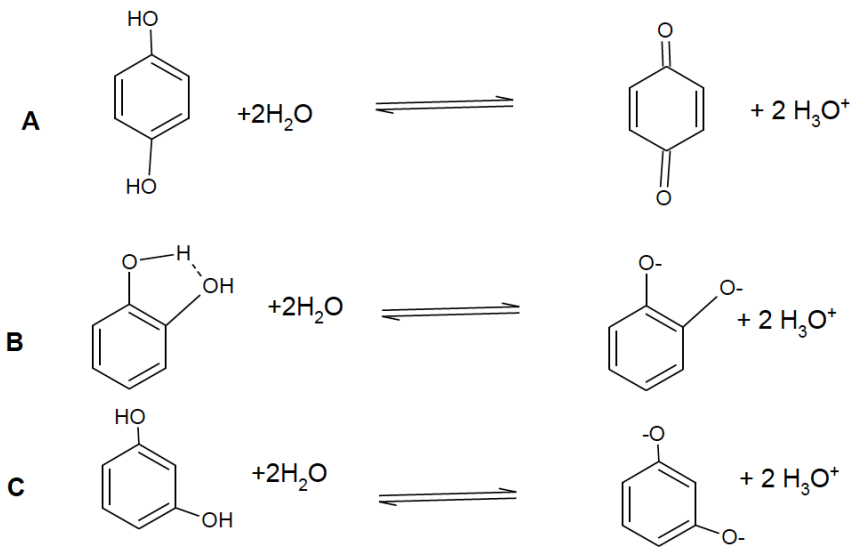

Figure 10: Proton transfer rate of the diphenols varies with the position of the phenolic groups. (**A**) 1,4 configuration of hydroquinone favors the formation of the stable benzoquinone which makes the fastest process. (**B**) Proximity effect in the 1,2 configuration of catechol facilitates intra-molecular hydrogen bonding, which reduces the bond-dissociation energy (BDE) of the phenolic bonds, thus facilitating their cleavage. (**C**) 1,3 configuration in resorcinol gives the slowest phenolic bond cleavage, leading to the slowest proton transfer rate and the lowest antioxidant capacity.

the formation of benzoquinone (Figure **10A**). Catechol, with a 1, 2 configuration of the two phenolic groups is ranked second. The relative ease of phenolic bond cleavage in catechol relative to resorcinol (1, 3 configuration) that was ranked third and lowest, is due to the proximity effect in catechol that permitted the formation of intra-molecular hydrogen bonding, with a resultant weakening of the phenolic bond (Figure **10B**). Resorcinol, with its 1, 3 configuration gave the lowest AOC because it possesses the strongest phenolic bonds, that are not easily cleaved (Figure **10C**).

The widely varied CAOCS values for the diphenol isomers (all having 2 unsubstituted phenolic groups) confirms our hypothesis that the chemical environment, which is underscored by the 'position' of the phenolic groups is critical to the AOC profiling. Arts *et al*. [13] reported the inaccuracy of the assay method, trolox equivalent antioxidant capacity (TEAC) in ranking the antioxidant capacity of the diphenol isomers. Resorcinol gave the highest TEAC value, yet its antioxidant capacity was reportedly inferior to that of catechol and hydroquinone in several other *in vitro* assays. This corroborates our findings that indicated resorcinol has the lowest antioxidant capacity and underscores the inconsistency and lack of SACC in some other assays.

Derivatives of hydroquinone have been prepared to enhance its antioxidant capacity. α-tocopheryl hydroquinone was reported as an efficient antioxidant compound [14]. t-butyl hydroquinone (TBHQ) is another derivative that has found application commercially. TBHQ has been compared with butylated hydroxyanisole (BHA) and butylated hydroxytoluene (BHT), and the ranking of their antioxidant capacity varies with the measurement methods [15].

Unfortunately, there is inconsistency in the values reported for the dissociation constant of the diphenols in literature [16]. Many sources report a single value for each of the diphenols, while another source documented two pKa values. The reported dissociation constants at 25^{o}C are; HQ (pK_1 = 9.85, pK_2 = 11.40); CTC (pK_1 = 9.34, pK_2 = 12.60) and RES (pK_1 = 9.32, pK_2 = 11.10) [17]. The total pKa values (pKa_T) are 21.25, 21.94 and 20.42 for HQ, CTC and RES respectively. pKa_T , which was previously shown to correlate with CAOCS metric, using a structurally diverse set of compounds [4], deviates from the usual correlation, with resorcinol producing the outlier data point. Previous attempts have shown relationships that exist between the chemical structures of polyphenols and their antioxidant activity. The flavonoids; quercetin, taxifolin and catechin, which possess different basic structures but the same hydroxylation pattern (Figure **2**), were shown to exhibit comparable antioxidant activities against different oxidants. The conclusion that the common catechol fragment is responsible for their antioxidant activity is however weakened by the finding that kaempferol, which has no catechol, but resorcinol

fragment, also shows high antioxidant activity. It was then observed that kaempferol has enolic hydroxyl group in common with quercetin [18]. It became obvious that SACC is an interplay of several structural factors and rather non-linear in nature [19]. In particular, studies on SACC concluded that the partition coefficients and the rate of reaction towards the relevant radicals define the antioxidant activity *in vivo* [20].

Several plant based polyphenols have higher antioxidant capacity than hydroquinone. As such, cosmetic preparations containing hydroquinone as active ingredient exhibited extended shelf life when stabilized by extracts of green tea [21]. Application of CAOCS assay to the manufacturing science of dietary supplements containing natural antioxidants is ongoing in our laboratory.

In sum, CAOCS assay incorporates real-time kinetics of phenolic bond cleavage and complete avoidance of any incubation period in AOC profiling. This assay thus conforms to a critical requirement for reliable AOC profiling, which is often overlooked, and represents the drawback of many previous chemical assays [22].

CONCLUSION

CAOCS assay results demonstrated that the antioxidant capacity for polyphenols, is dependent on the number of unsubstituted phenolic groups and more importantly, on the 'position' (chemical environment) of the phenolic groups. 250 µL increments up to a maximum of 1.75 mL were shown to be the preferred protocol for the photometric assays. This modification will ensure 75% reduction in the amount of active material required for the assay, relative to existing protocol that uses 1 mL increments. This significant reduction in cost of analysis makes the CAOCS assay attractive for profiling more expensive polyphenols. A low-cost assay, which holds a great promise for quality-by-design (QbD), was thus optimized for polyphenols. Further refinement of the assay protocol, by using yet smaller increment (i.e. < 250 µL) and chemoinformatics approach of integrating lipophilicity measurement with CAOCS metric is being investigated in our laboratory to provide a more robust characterization of biorelevant antioxidant capacity.

ACKNOWLEDGEMENTS

The authors thank Mr. Bidemi Bello and Mr. Joseph Keshinro for their technical assistance. This work was funded by Senate Research Grant #: SRG/FP/2010/2A awarded to SOI, by the Senate Research Grants Committee, University of Ibadan, Ibadan, Nigeria.

REFERENCES

[1] Apak R, Gorinstein S, Böhm V, Schaich KM, Özyürek M, Güçlü K. Methods of measurement and evaluation of natural antioxidant capacity/activity (IUPAC Technical Report). Pure Appl Chem 2013; 85: 957-98. http://dx.doi.org/10.1351/PAC-REP-12-07-15

[2] Haytowitz D, Bhagwat S. USDA Database for the Oxygen Radical Absorbance Capacity (ORAC) of Selected Foods [monograph on the internet]. Maryland: U. S. Department of Agriculture 2010; 10-48.

[3] USDA. Oxygen Radical Absorbance Capacity (ORAC) of Selected Foods, Release 2 (2010).

[4] Idowu SO. Computational antioxidant capacity simulation (CAOCS): a novel framework of antioxidant capacity profiling. Chem Prod Process Model 2014; 9: 25-43. http://dx.doi.org/10.1515/cppm-2013-0041

[5] Idowu SO, Adeyemo MA, Itiola AJ. Computational models for the determination of antioxidant capacity and phenolics in dietary supplements using real-time proton transfer kinetics data. Chem Prod Process Model 2009; 4(1). [serial on the internet]. 2009 Oct 14; [cited 2016 Sept 9]. Available from: http://www.degruyter.com/view/j/cppm.2009.4.1/cppm.2009.4.1.1385/cppm.2009.4.1.1385.xml?format=INT

[6] Rosch D, Bergmann M, Knorr D, Kroh LW. Structure-antioxidant efficiency relationships of phenolic compounds and their contribution to the antioxidant activity of sea buckthorn juice. J Agric Food Chem 2003; 51: 4233-9. http://dx.doi.org/10.1021/jf0300339

[7] Nihro Y, Furukawa H, Sogawa S, *et al*. Synthesis and anti lipid-peroxidation activity of hydroquinone monoalkyl ethers. Chem Pharm Bull (Tokyo) 1994; 42: 576-9. http://dx.doi.org/10.1248/cpb.42.576

[8] Yamaguchi LF, Lago JHG, Tanizaki TM, Mascio P Di, Kato MJ. Antioxidant activity of prenylated hydroquinone and benzoic acid derivatives from Piper crassinervium Kunth. Phytochemistry 2006; 67: 1838-43. http://dx.doi.org/10.1016/j.phytochem.2006.03.001

[9] Akaike H. A New Look at the Statistical Model Identification. IEEE Trans Automat Contr 1974; 19: 716-23. http://dx.doi.org/10.1109/TAC.1974.1100705

[10] Willard HH, Merrit Jr LL, Dean JA, Settle Jr FA. Ultraviolet and visible absorption methods. Instrumental Methods of Analysis. 7th ed. California: Wadsworth Publishing Company; 1988; pp. 159-76.

[11] Martin A. Complexation and Protein binding. Physical Pharmacy. 4th ed. Baltimore: Lippincot Williams & Wilkins; 1993; pp. 254-7.

[12] Chang R. Acids and Bases. General chemistry: the essential concepts. 3rd ed. Boston: McGraw Hill; 2003; pp. 501-32.

[13] Arts MJTJ, Dallinga JS, Voss HP, Haenen GRMM, Bast A. A critical appraisal of the use of the antioxidant capacity (TEAC) assay in defining optimal antioxidant structures. Food Chem 2003; 80: 409-14. http://dx.doi.org/10.1016/S0308-8146(02)00468-5

[14] Neuzil J, Witting PK, Stocker R. α-tocopheryl hydroquinone is an efficient multifunctional inhibitor of radical-initiated oxidation of low density lipoprotein lipids. Proc Natl Acad Sci USA 1997; 94: 7885-90. http://dx.doi.org/10.1073/pnas.94.15.7885

[15] Karamac M, Amarowicz R. Antioxidant activity of BHA, BHT and TBHQ examined with Miller's test. Grasas y Aceites 1997; 48: 83-6. http://dx.doi.org/10.3989/gya.1997.v48.i2.772

[16] Yin HS, Zhang QM, Zhou YL, *et al*. Electrochemical behavior of catechol, resorcinol and hydroquinone at graphene-chitosan composite film modified glassy carbon electrode and their simultaneous determination in water samples. Electrochim Acta 2011; 56: 2748-53. http://dx.doi.org/10.1016/j.electacta.2010.12.060

[17] Sober HA, Ed. CRC Handbook of Biochemistry. CRC Press, Boca Raton, FL; 1968.

[18] Silva MM, Santos MR, Caroco G, Rocha R, Justino G, Mira L. Structure-antioxidant activity relationships of flavonoids: a re-examination. Free Radic Res 2002; 1219-27. http://dx.doi.org/10.1080/198-1071576021000016472

[19] Di Majo D, Giammanco M, La Guardia M, Tripoli E, Giammanco S, Finotti E. Flavanones in Citrus fruit: Structure-antioxidant activity relationships. Food Res Int 2005; 38(10): 1161-6. http://dx.doi.org/10.1016/j.foodres.2005.05.001

[20] Rice-Evans CA, Miller NJ, Paganga G. Structure-antioxidant activity relationships of flavonoids and phenolic acids. Free Rad Biol Med 1996; 20: 933-56. http://dx.doi.org/10.1016/0891-5849(95)02227-9

[21] Morteza-Semnani K, Saeedi M, Nozadi Z. Comparison of antioxidant activity of extract of Green tea to commercial antioxidants in 2% hydroquinone cream. J Med Plants 2005; 1: 36-45. 2014 Dec 8.[cited 2016 Sept 9]. Available from: http://www.jmp.ir/browse.php?a_id=716&sid=1&slc_lang=en

[22] Schaich KM, Tian X, Xie J. Reprint of Hurdles and pitfalls in measuring antioxidant efficacy: A critical evaluation of ABTS, DPPH, and ORAC assays. J FunctFoods 2015; 18: 782-96. http://dx.doi.org/10.1016/j.jff.2015.05.024

Received on 08-05-2016 Accepted on 07-09-2016 Published on 17-10-2016

DOI: http://dx.doi.org/10.6000/1929-5030.2016.05.03.5